
Solid state systems for quantum information, Correction 11

Assistants : franco.depalma@epfl.ch, filippo.ferrari@epfl.ch

Exercise 1 : Optimizing the measurement setup

1. The need of attenuation:

The blackbody radiation present in cables depends on the temperature of a resistor R connected to them. To see this, let us consider a bath at temperature T . The temperature-dependent mean thermal photon occupation number n_{BE} of the bath at a given frequency $\omega/2\pi$ is given by the Bose-Einstein distribution:

$$n_{BE} = \frac{1}{\exp\left(\frac{\hbar\omega}{k_B T}\right) - 1}. \quad (1)$$

Placing an attenuator that reduces the power of the signal by a factor A , at a temperature stage T , one relates the input noise photon occupation n_i to the output noise photon occupation n_o at frequency ω by the following rule:

$$n_o(\omega) = \frac{n_i(\omega)}{A} + \frac{A-1}{A}n_{BE}(T, \omega). \quad (2)$$

This is to be thought of as a beam-splitter letting $1/A$ of the signal go through, and adding $(A-1)/A$ of the thermal emission from a bath at temperature T .

(a) What is the classical limit of Eq.1?

Hint: Consider $\hbar\omega \ll k_B T$ and apply a first-order Taylor approximation in the denominator.

(b) Estimate the amount of total attenuation (starting from room temperature) needed to reach a noise level of $n_{th} = 10^{-3}$ at a frequency of 6 GHz at the input of the sample, which has a temperature of 20 mK. Assume that the noise at room temperature is dominated by thermal noise.

(c) What limits the amount of attenuation that can be used in practical experiments? We typically distribute 60 dB of attenuation between the 4 K stage, the cold plate at 100 mK, and the base temperature stage at 20 mK. What is the noise photon number you get for a 20/20/20 dB attenuator distribution at a frequency of 6 GHz?

(d) For each of the attenuators, plot the noise photon occupation number at a frequency of 6 GHz at the input of the sample as a function of the attenuation if the other two attenuators are fixed to 20 dB? Explain your observations.

2. Noise in the amplification chain:

We consider the amplification chain sketched in Fig. 1, which is used to amplify signals on their way from the superconducting chip towards the room temperature acquisition device. The chain consists of 1) an effective attenuator with attenuation constant A taking into

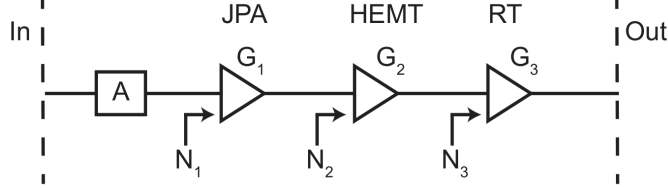


Figure 1: Sketch of an amplification chain with 3 stages.

account cable losses, 2) a Josephson Parametric Amplifier (JPA), 3) a High-Electron Mobility Transistor (HEMT) amplifier, and 4) a room temperature (RT) amplifier. Each amplifier has a gain G_i , as well as an added noise N_i specifying the effective number of noise photons at the input of the amplifier (the JPA's added noise is often negligibly small). The noise is given in terms of photons according to the table below.

Amplifier	Gain(dB)	Noise added
JPA	$G_1 = 20$	$N_1 \ll 1$
HEMT	$G_2 = 40$	$N_2 = 14$
RT amp.	$G_3 = 40$	$N_3 = 174$

The recorded signal is of the form $S = a + h^\dagger$. Without any input signal, the noise measured at the output of the chain is $\langle hh^\dagger \rangle = 1 + N_{\text{eff}}$.

- Write an equivalent single amplifier model with the effective gain G_{eff} and the effective input noise N_{eff} of the whole chain. Demonstrate that in the limit of large gain of the first amplifier, the effective noise figure is dominated by the noise of the first amplifier.
Hint: Assume that the attenuator A adds one noise photon due to vacuum noise.
- Estimate the chain efficiency $\eta = \frac{1}{1+N_{\text{eff}}}$ for $A = 1$ dB. How close is it to being quantum limited?

Solution 1 :

1. The need of attenuation:

- The classical limit corresponds to $\hbar\omega \ll k_B T$, that is, the discrete photon energy is small compared to the spread imposed by temperature. We Taylor-expand the exponential of a small number x as $\exp(x) \approx 1 + x$ to find the Maxwell-Boltzmann distribution

$$n_{BE} = \frac{1}{\exp\left(\frac{\hbar\omega}{k_B T}\right) - 1} \approx \frac{k_B T}{\hbar\omega} = n_{\text{MB}}. \quad (3)$$

(b) We estimate the required attenuation by evaluating Eq. 2. Since $n_{\text{BE}}(20 \text{ mK}, 2\pi \cdot 6 \text{ GHz}) \approx 5.6 \cdot 10^{-7}$, we can ignore the second term of Eq. 2. To reach $n_{th} = 10^{-3}$ at 6 GHz, where the input from room temperature (ca. 300 K) corresponds to $n_i = n_{\text{BE}}(300 \text{ K}, 2\pi \cdot 6 \text{ GHz}) \approx 1000$ photons, we need

$$A \approx 10^6 = 60 \text{ dB} \quad (4)$$

(c) The heat load due to signal dissipation, compared to the cooling power in the cold stages of the dilution refrigerator, is the limiting factor. Placing a 60 dB attenuator at the 20 mK stage would, for example, introduce a heat load far larger than the cooling power at that temperature stage. To reduce heat load at the low temperature stages due to signal dissipation, one distributes the total attenuation across the different temperature stages. A common choice is to put 20 dB attenuators at the 4 K, 100 mK and 20 mK stage.

We first evaluate the Bose-Einstein distribution at each attenuation stage, expecting $n_{300 \text{ K}} = 10^3$, $n_{4 \text{ K}} = 10^1$, $n_{0.1 \text{ K}} = 6 \cdot 10^{-2}$, $n_{0.02 \text{ K}} = 6 \cdot 10^{-7}$ noise photons for the temperatures 300 K, 4 K, 0.1 K, 0.02 K. Using Eq. 2, we see that the number of noise photons reaching the chip is equal to

$$((n_{300 \text{ K}}/100 + n_{4 \text{ K}})/100 + n_{0.1 \text{ K}})/100 + n_{0.02 \text{ K}} \approx 3 \cdot 10^{-3}. \quad (5)$$

(Here, we approximated $(A - 1)/A = 99/100 \approx 1$.)

(d) The result is shown in Fig. 2 Note: One notices that adding attenuation improves the

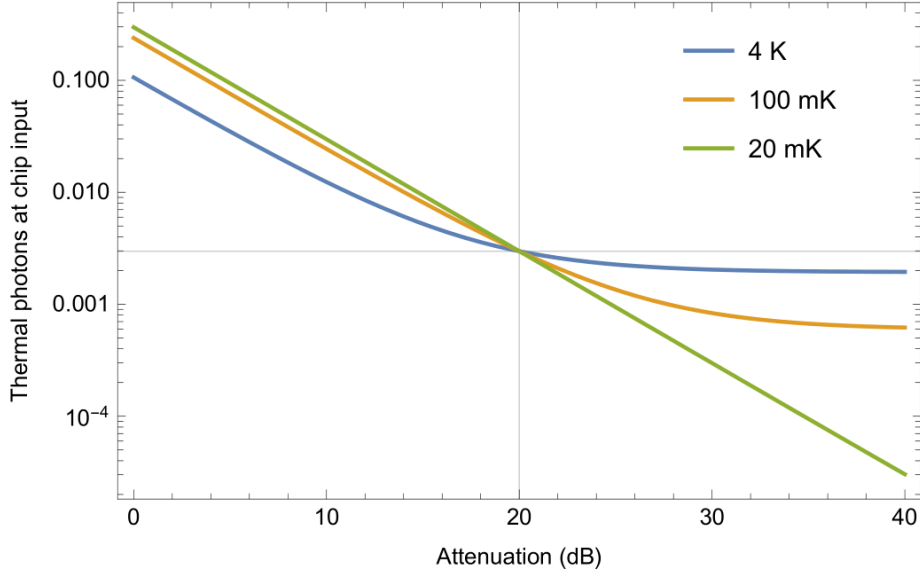


Figure 2: Calculated thermal photon number at the input of the chip as a function of the attenuation at the 4 K stage (blue), 100 mK stage (orange) and 20 mK stage (green) for a fixed attenuation of 20 dB at the respective other stages.

result only up to a threshold, which depends on the stage at which this attenuation is added. Above the threshold the input noise is already lower than the Bose-Einstein

occupation, and adding more attenuation does not decrease the noise level. A similar plot is contained in Krinner et al., EPJ Quantum Technol. **6**, (2019) as Fig. 2(a).

2. Noise in the amplification chain:

(a) The signal is reduced by the attenuator, and amplified in three stages as follows:

$$S_{out} = S_{in}G_{\text{eff}}, \quad (6)$$

where $G_{\text{eff}} = A^{-1}G_1G_2G_3$ is the effective gain of the whole chain.

The noise from each stage is amplified by the following stages, and they add up to the output noise:

$$N_{out} = ((A - 1)/A + N_1)G_1G_2G_3 + N_2G_2G_3 + N_3G_3. \quad (7)$$

Note that we accounted for the vacuum noise added by the attenuator. (At finite temperature, an attenuator adds $(A - 1)/A n_{\text{BE}}(T, \omega)$ of noise (see Problem 1.1). At 20 mK and 6 GHz, $n_{\text{BE}}(T, \omega) \approx 10^{-7}$, but the attenuator still adds at least one photon from vacuum fluctuations.)

We refer the noise to the input of the chain by dividing the output noise by G_{eff} :

$$N_{\text{eff}} = A - 1 + N_1A + N_2\frac{A}{G_1} + N_3\frac{A}{G_1G_2}. \quad (8)$$

Importantly, aiming to keep the signal to noise ratio close to that of the input requires to have the amplified noise of the earlier stages surpassing already the added input noise of the following stage. Using a quantum-limited amplifier where N_1 is close to zero, this means that we require $\frac{N_2A}{G_1} \ll A - 1$ and similarly $\frac{N_3A}{G_1G_2} \ll A - 1$. This is achieved in the limit of large gain G_1 .

(b) The effective noise referred to the input of the chain is $N_{\text{eff}} = 10^1/10 \cdot (1 + 14/10^2 + 174/10^6) - 1 = 0.43$ photons. The efficiency is $\eta = 70\%$, close to being quantum-limited (limit of 1 given by the vacuum fluctuations).

Note: The efficiency determines the number of averaging that is required in an experiment to reach a given statistical standard deviation. The scaling for an amplitude measurement is that the standard deviation Δ decreases linearly with the efficiency, and with the square root of the number of times N a given measurement was repeated: $\Delta \propto \frac{1}{\eta\sqrt{N}}$

Exercise 2 : Microwave pulse generation by frequency upconversion

As discussed in the lecture and some of the previous problem sets, single-qubit manipulation is achieved by applying a voltage pulse $V_p(t)$ to the qubit drive line which oscillates at a frequency resonant with the qubit transition frequency ω_{ge} . A typical functional form for such pulses reads

$$V_p(t) = V_0 e^{-(t/\tau)^2} \cos(\omega_{ge}t + \phi), \quad (9)$$

where $\omega_{ge} = 2\pi \cdot 6$ GHz and $\tau = 5$ ns. Voltage pulses couple to the qubit via dipole-field interactions where the phase ϕ of the driving field is used to control the axis about which the Bloch vector of the qubit is rotated.

1. To generate voltage pulses with a controlled envelope, e.g. the Gaussian envelope $V_p(t)$, we use an arbitrary waveform generator (AWG) with a sampling rate of 1.2 GS/s. What is the maximum bandwidth of a signal that can be generated by such an instrument?
2. To generate pulses in the GHz regime, one typically uses a frequency mixer, which can multiply two signals. Usually, one multiplies the signal generated by the AWG at an intermediate frequency (IF) with a continuous local oscillator (LO) field generated by a microwave generator running at GHz frequency, see schematic Fig. 3(a).

Derive the output signal when applying a continuous frequency of $\omega_{LO} = \omega_{ge} + \omega_{IF} = 2\pi \cdot 6.2$ GHz to the LO port and the pulse $V_p(t) = V_0 e^{-(t/\tau)^2} \cos(\omega_{IF}t + \phi)$ with $\omega_{IF} = 2\pi \cdot 200$ MHz to the IF port. Calculate the Fourier transform, and plot its absolute value in the frequency domain. What issue do you see when using the upconverted signal to drive the qubit?

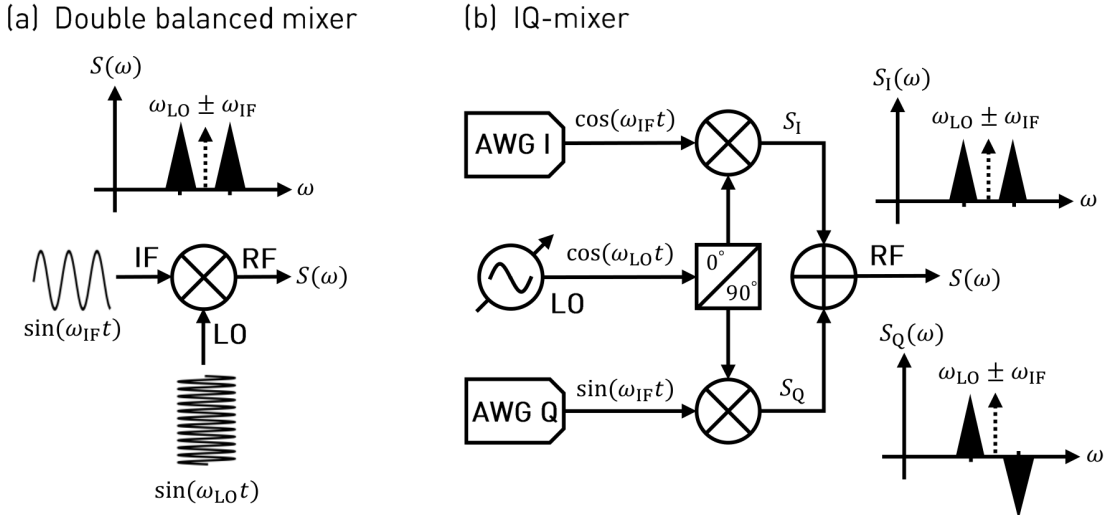


Figure 3: Conventional double balanced mixer, for which the output signal at the RF port is the product of the signals at the IF and LO port. (b) IQ-mixer, which is composed of two double balanced mixers, a 90° hybrid splitter, and a microwave combiner. The hybrid splitter divides the incoming LO signal equally and adds a 90° phase shift for the LO to the quadrature mixer, such that the signal results in $\cos(\omega_{LO}t - \pi/2)$.

3. To avoid the generation of two sidebands at frequencies $\omega_{\text{LO}} \pm \omega_{\text{IF}}$, we perform two upconversion processes, according to the IQ-mixing scheme shown in Fig. 3(b). Show that one of the two sidebands is effectively eliminated in the signal $S(\omega)$. What is the motivation for letting the experimentalist provide the two IF signals I and Q independently instead of generating the Q input internally in the IQ-mixer by phase-shifting the I input?
4. A drive pulse at the same frequency ω_{ge} can also be created with $\omega_{\text{LO}} = 2\pi \cdot 5.8 \text{ GHz}$. How do the I and Q input signals need to be modified in this case?
5. We now consider the acquisition of the microwave pulses for the readout of the qubit state. In the readout output line, the bandwidth of the signal acquisition is limited by the sampling rate of the analog to digital converter (ADC). Describe briefly how the IQ-mixer from Fig. 3(b) can be used to convert the readout signal from the GHz band down to frequencies within the bandwidth of the ADC?

Solution 2 :

1. The highest frequency one can generate in the baseband is realized by outputting a string of $\{V, -V, V, -V, \dots\}$. This corresponds to a frequency of half the sampling rate, which is called the Nyquist frequency and is 600 MHz in this case.
2. We take a continuous wave voltage of the form $V_{\text{LO}}(t) = V_{\text{LO}} \cos((\omega_{ge} + \omega_{\text{IF}})t)$ at the LO port and calculate its product with the IF signal $V_p(t)$ using the trigonometric identity: $\cos(x) \cdot \cos(y) = \frac{1}{2} (\cos(x - y) + \cos(x + y))$,

$$V_{\text{RF}} = V_p(t) \cdot V_{\text{LO}}(t) = \frac{V_0 V_{\text{LO}}}{2} e^{-(t/\tau)^2} (\cos(\omega_{ge}t - \phi) + \cos((\omega_{ge} + 2\omega_{\text{IF}})t + \phi)). \quad (10)$$

The first cosine terms corresponds to the upconverted pulse at the targeted frequency ω_{ge} , the second term is referred to as the opposite sideband. Let us call its frequency $\omega_r = \omega_{ge} + 2\omega_{\text{IF}}$ to simplify the notation later.

As the cosine function can be written as the sum of two complex exponentials, $\cos(x) = \frac{e^{ix} + e^{-ix}}{2}$, the Fourier transform of the cosines in Eq. 10 yields delta peaks at positive and negative frequencies

$$\mathcal{F}\{\cos(\omega_0 t + \phi)\} = \frac{1}{2} [e^{i\phi} \delta(\omega + \omega_0) + e^{-i\phi} \delta(\omega - \omega_0)] \quad (11)$$

The Fourier transform of a product of two terms in the time domain is the convolution of the individual Fourier transforms in the frequency domain,

$$\mathcal{F}\{S_1(t) \cdot S_2(t)\} = \mathcal{F}\{S_1(t)\} \cdot \mathcal{F}\{S_2(t)\}. \quad (12)$$

The Fourier transform of the Gaussian envelope remains a Gaussian up to rescaling

$$\mathcal{F}\{e^{-(t/\tau)^2}\} = \sqrt{\pi\tau^2} e^{-(\tau\omega/2)^2}. \quad (13)$$

Using Eq. 12 with $S_1(t)$ being the Gaussian envelope from Eq. 13 and $S_2(t)$ the sum of both cosines at frequencies ω_{ge} and ω_r from Eq. 11, we find that the Fourier transform of Eq. 10 is

$$\mathcal{F}\{V_{\text{RF}}\} = \frac{V_0 V_{\text{RF}}}{2} \frac{\sqrt{\pi\tau^2}}{2} \left[e^{-\phi-\tau^2(\omega-\omega_{ge})^2/4} + e^{\phi-\tau^2(\omega+\omega_{ge})^2/4} + e^{-\phi-\tau^2(\omega-\omega_r)^2/4} + e^{\phi-\tau^2(\omega+\omega_r)^2/4} \right]. \quad (14)$$

We plot the absolute value of the spectrum $\mathcal{F}\{V_{\text{RF}}\}$ in Fig. 4 for positive frequencies and observe two Gaussian distributions centered around frequencies $\pm\omega_{ge}$ and $\pm\omega_r$. Since the frequency of the opposite sideband is very close to the actual qubit transition frequency ω_{ge} , its presence will introduce significant errors in the control of the qubit state. Removing it by a filter is technically almost impossible.

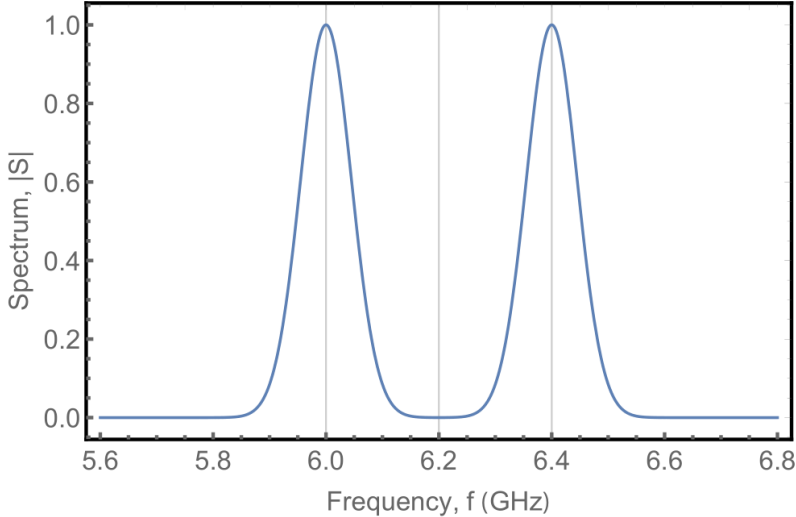


Figure 4: Absolute value of the Fourier transform of $V_{\text{RF}}(t)$ vs frequency. The gridlines indicate (from left to right) ω_{ge} , $\omega_{\text{LO}} = \omega_{ge} + \omega_{\text{IF}}$ and $\omega_{ge} + 2\omega_{\text{IF}}$.

3. We calculate the output of the mixers at the I-port and the Q-port, $V_I(t)$ and $V_Q(t)$, respectively, using the trigonometric identity from 2. and $\sin(x) \cdot \sin(y) = \frac{1}{2} (\cos(x-y) - \cos(x+y))$,

$$V_I(t) = \cos(\omega_{\text{LO}}t) \cdot \cos(\omega_{\text{IF}}t) = \frac{1}{2} [\cos((\omega_{\text{LO}} - \omega_{\text{IF}})t) + \cos((\omega_{\text{LO}} + \omega_{\text{IF}})t)] \quad (15)$$

$$V_Q(t) = \sin(\omega_{\text{LO}}t) \cdot \sin(\omega_{\text{IF}}t) = \frac{1}{2} [\cos((\omega_{\text{LO}} - \omega_{\text{IF}})t) - \cos((\omega_{\text{LO}} + \omega_{\text{IF}})t)]. \quad (16)$$

From Eq. 16, it is easy to see that by combining V_I and V_Q , the sideband at frequency $\omega_{\text{LO}} + \omega_{\text{IF}}$ will be eliminated and the output of the RF port has only the desired frequency component

$$V_{\text{RF}}(t) = V_I + V_Q = \cos((\omega_{\text{LO}} - \omega_{\text{IF}})t). \quad (17)$$

In general, manufacturers let the user of the mixer provide the two quadratures independently, as this allows to compensate for imperfections such as uncalibrated phase offsets in the two signal paths of the IQ-mixer.

4. To generate the drive pulse with $\omega_{\text{LO}} = 2\pi \cdot 5.8$ GHz, we need to eliminate the opposite sideband as in 3. This can easily be achieved by inverting the sign of the IF modulation signal at either the I or Q input, such that

$$V_{\text{RF}}(t) = V_{\text{I}} + V_{\text{Q}} = \cos((\omega_{\text{LO}} + \omega_{\text{IF}})t). \quad (18)$$

5. Downconversion is the inverse process to frequency upconversion, where we use the RF and LO port of the mixer as inputs. We choose the frequency detuning of the LO to the readout signal applied to the RF port such that the downconverted IF signals are within the bandwidth of the ADC. The readout signal at GHz frequency gets converted down to the MHz band where room temperature electronics can now digitize it and record the result of our quantum measurement.